Inspection and Verification of 3D Laser Scanning Datasets Registration for Reverse Engineering Application, Part 1: A Product with Datum

Muslimin [1], Jiang Zhua [2], Hayato Yoshioka [3], Tomohisa Tanaka [4]

[1, 2, 3] *Department of Mechanical and Control Engineering*, Tokyo Institute of Technology, Japan.
[1] *Department of Mechanical Engineering*, Politeknik Negeri Jakarta, Indonesia.
[4] *Department of Micro-Nano System Engineering*, Nagoya University, Japan.

[1] Corresponding Author E-mail: muslimin@mesin.pnj.ac.id

Abstract - Registration of point cloud datasets from a laser scanner is crucial in pursuing an accurate product in the reverse engineering. In practice, dataset error and registration error are the main sources of failure in achieving an accurate registration result. The lack of the inspection method of registration result becomes a challenge in guaranteeing the accuracy. This paper presents a novel method of the inspection and verification of point clouds registration to minimize the registration errors. In this method, aligned point clouds are inspected and verified using data from a CMM taken in correspondence with pre-defined object features. Point cloud segmentation and feature extraction are utilized to define concerned features while a grid method is used to perform the correspondence between the considered feature and CMM dataset. The method was implemented into a real case product to analyze its reliability. Based on the implementation, the proposed method showed the effectiveness in inspecting and verifying the registration result.

Keywords - 3D CAD model, point cloud datasets, CMM data set, registration, feature extraction, feature inspection

I. INTRODUCTION

In a laser or optic scanning, scanning process is often applied in some different positions to obtain complete surface data of an object. The registration process is applied to unify the acquired datasets. Generally, the registration process is implemented in two steps: rough and fine registration [1-3]. Rough registration is used to align transformed data onto reference data while fine registration is used to refine the pairwise datasets fitting [1]. Furthermore, the final datasets obtained from the registration is used to construct a 3D-CAD model.

The current problem of the registration of point cloud datasets is the lack of guarantee of accuracy and precision. Deviation (error) of the registration of point cloud datasets is necessarily controlled to assure 3D-CAD model construction conforms to the reversed object. The registration error is able to be traced according to its error sources. In practice, there are two major error sources: dataset error and registration error. Dataset error is the error within a single dataset which is produced by scanning process flaws such as noise, holes, shift and the other improper data [4]. On the other hand, the registration error is the failure to get the best alignment and fitting between the registered datasets. Both of the error types influence the accuracy of CAD model construction and furthermore affect the precision of the duplicated object.

In the conventional reverse engineering, a prototype is developed regarding to the constructed CAD model to check the accuracy of a duplicated object. The dimensional geometry of the prototype is measured and compared to the dimensional geometry of the reversed object. Repetitive processes are applied until the sophisticated result is achieved. This process is uneconomical thus effort is made to encompass a process in which the inspection and verification are applied from the registration process. The point cloud datasets and the registration result are simultaneously inspected and verified using coordinate measuring machine (CMM) data. Correction of the registration and datasets can be performed based on the error evaluation.

This paper proposes the method of inspection and verification of the point clouds registration from laser scanning using CMM data. The main aim is to assure that the 3D CAD model constructed from laser scanning datasets conforms to the reversed object. In this proposed method, aligned point clouds are inspected and verified using data from a CMM taken in correspondence with pre-defined object features. The accuracy of the registration is evaluated based on the inspection and verification from overall pre-defined single features. Segmentation and feature extraction [2, 5, 6] are implemented to extract each features from the point cloud. A grid method [1, 7] is used to form the correspondence between the considered feature and CMM dataset. The inspection and verification of each feature are then applied in each related grid.

This work has three prospective contribution objectives. First is to develop a model for inspecting and verifying the point clouds registration from other scanner devices. Second is to develop a method of registration for different data types

such as a point cloud dataset and a discrete dataset from various measurement devices and datasets with different density. Third is to study a hybrid method of the registration and the inspection simultaneously. This approach can be applied in reverse engineering of a wide variety of products such as mechanical, molding, casting, forging products and so on.

II. RELATED WORK

The laser scanner is an electro-optical device that is popular to acquire dense point dataset of an object surface in very short time, suitable for measuring both regular and irregular surfaces, and viable to build up an accurate 3D CAD model [1-3]. This device works based on the optical triangulation in which the object geometry and its measurement position will affect the quality of the retrieved dataset [8]. However, because of its natural characteristics and scanning condition, some errors such as noise, hole, shift and the other improper data are unable to be avoided in scanning process [9-11]. This error can be minimized regarding to its sources.

Feng, et al [10] examined the combination of random error and systematic error resulting in digitizing error of a laser scanner. Random error occurs from some sources such as surface reflectivity, color, contour and so on which are difficult to control while systematic error occurs from controlled parameters such as scan depth, incident angle and projected angle [9-11]. Correction of systematic error of laser scanning devices to improve the accuracy was proposed by Isheil et al. [9]. The evaluation tests of the laser scanners performance on CMMs are suggested by Gestel et al. [11]. However, in practice, these errors are very difficult to be avoided.

The registration of point cloud datasets plays a significant role in determining the accuracy of the constructed CAD model from the laser scanning. Some efforts have been done to obtain more accurate registration result [1-3, 9-10]. However, due to the lack of error inspection in the registration result, the accuracy of duplicated 3D CAD cannot be guaranteed. Moreover, due to the limited references discussed the inspection and verification of registration result and most existing methods focused on the inspection of the final product [7], the inspection of registration result is very crucial in the reverse engineering using a laser scanner since the complexity, accuracy, and precision of reversed parts increase.

A coordinate measuring machines (CMM) is high accurate measurement device in spite of more time-consuming. Naturally, CMM has measurement error caused by the sensitivity of probe diameter, probing speed, material condition, and operator skill [11]. ISO 10360-2 [12] specifies the verification guide line to determine CMM performance conform to errors. Nevertheless, CMM is still much more accurate than the current laser scanner. Therefore, the CMM can be used to inspect and verify point cloud datasets from a laser scanner.

Carbone, et.al [13] used a CMM to inspect a rough CAD model that resulted from vision data registration for reverse engineering of the freeform surface. However, the lack of information of each single extracted feature in this system makes that proposed method cannot be used to trace the source of registration error.

In our proposed method, CMM data is used to inspect and verify each pre-defined key features which are extracted from the point cloud and from which the registration error is evaluated. Based on the evaluation, the source of registration error can be traced from its sources: point cloud error, registration error, or the combination of them. Examples of the point cloud error in a cylinder and parallel planes are shown in Fig. 1 (a) and Fig. 1(b), respectively [1] while an example of the registration error in a cylinder is shown in Fig. 2.

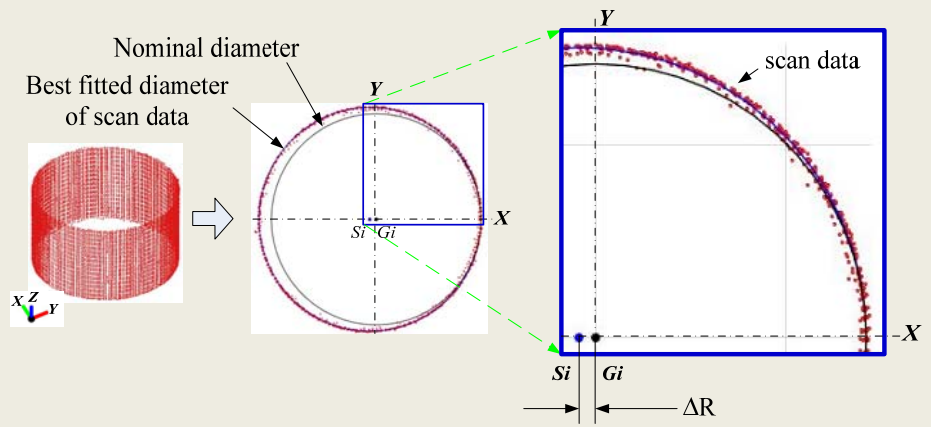

(a), Figure 1 continues on next page

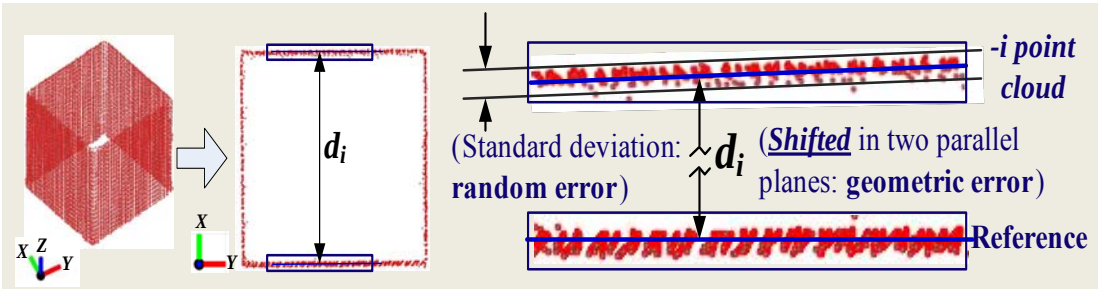

(b)

Fig. 1 Examples of dataset error: (a) dataset error obtained from the laser scanning of a cylinder, and (b) dataset error obtained from the scanning of two parallel planes. G-i is a nominal center of a cylinder, S_i is a new center of point cloud dataset and ΔR is deviation value, and d-i is deviation along parallel planes.

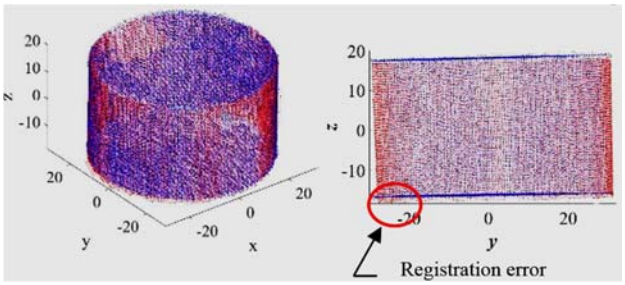

(a) (b)

Fig. 2 An Example of the registration error: (a) 3D view, and (b) 2D view (y-z axis)

In the inspection and verification of registration result, point cloud data needs to be converted into definitive features. Segmentation and feature extraction [2, 5, 6] are applied to obtain the information about the topology and geometrical property of the extracted features from the point cloud datasets. In this proposed method, each single extracted feature is then identified and classified. Verification is carried out to verify each feature such as a point, group of points, line, plane, cylinder, ruled surface and free form surfaces. The extracted features are then utilized as considered features in which the inspection and verification using CMM data are performed.

The main concerns of this paper were inspection and verification of the point clouds registration from the laser scanner. Inspection as well as verification of each extracted feature is implemented by evaluating each corresponding point cloud and CMM points in localized grids. The geometrical error of an extracted feature is estimated based on the deviation of the Euclidian distance between point cloud and CMM point in all related grids [1,7]. The Euclidian distance can be determined by the distance deviation of plane-to-plane, plane-to-point, and point-to-point. The inspection result is statistically verified and analysed to make a sophisticated correction.

III. THE PROPOSED METHOD

A. Examination of Reversed Object and Inspection Planning

This first step aims to collect all relevant information and to determine the appropriate processes and devices. General information such as physical condition, function, material, manufacturing, assembly, size and so on are gathered from an object. Main features of the object such as plane, cylinder, edge, curve and free-form surfaces are identified. Regarding to the function, pre-defined features product can be classified into critical (key) and non-critical (non-key) features. Although both critical and non-critical features are important to assure the functionality of the product, the only concern lies in the critical features to be inspected and verified because they directly influence the product function. The planning of laser scanning and CMM measurement are developed according to the pre-defined feature. In this step, the number and position of CMM points of each feature and the position of laser scanning are assigned. The decision of selecting datum or corresponding features or attaches regular shapes, such as rectangular or cylinder shapes, to the object as measurement references is also established.

Let F_w be a key feature w, for $w = 1,2,\dots,W$, where W is the number of critical features to be inspected, and D_ω be a datum ω (for the object with datum), for $\omega = 1,2,\dots,M$, where M is the number of datum features used as the inspection references. E_{F_w} and E_{D_ω} are extracted features corresponding to key features (F_w) and datum features (D_ω), respectively. I_{F_w} and I_{D_ω} are the CMM point dataset which are used to inspect the extracted features, E_{F_w} and E_{D_ω}, respectively. c_{F_w} and c_{D_ω} are the number of the CMM points retrieved in the CMM dataset, I_{F_w} and I_{D_ω} to inspect the extracted features, E_{F_w} and E_{D_ω}, respectively. The inspection planning is identified as shown in Table I.

TABLE I. THE PLANNING OF FEATURES INSPECTION

Features (F_w)	Extracted features (E_{F_w})	Related datum features, D_ω	CMM data point for inspection	
			Inspected point dataset (I_{F_w})	Number CMM points (c_{F_w})
F_1	E_{F_1}	D_ω	I_{F_1}	c_{F_1}
F_2	E_{F_2}	D_ω	I_{F_2}	c_{F_2}
. .	. .	…	. .	. .
F_W	E_{F_W}	D_ω	I_{F_W}	c_{F_W}

B. CMM Measurement

The number of CMM points and their position related to each pre-defined feature are depending on the complexity and level of accuracy. The number of CMM points retrieved and its position in each feature must convince its feature geometry property and also still economically. The number of CMM points retrieved and their position will also influence the accuracy and validity of the measurement.

Based on the measurement planning, let $p_{c_{w,u}}$ be a set of CMM point using to inspect the extracted feature,E_{F_w}, for $u = 1,2, \dots, c_{F_w}$. The CMM point which is retrieved from a certain feature, E_{F_w} $(\text{or } E_{D_\omega})$, is a member of the CMM dataset, $p_{c_{w,u}} \epsilon\ I_{F_w}$ (see Table 1 above). Each CMM point, $p_{c_{w,u}}$ of I_{F_w} will be used to inspect and validate the extracted feature, E_{F_j}. The correspondence between an extracted feature, E_{F_w} and the inspected CMM points, $\forall p_{c_{w,u}} \epsilon\ I_{F_w}$ for pre-defined features is formulated as follows:

$$F_w \approx E_{F_w} \approx I_{F_w}\left[p_{c_{w,1}}, p_{c_{w,2}}, \dots, p_{c_{w,c_{F_W}}}\right] \quad (1)$$

where E_{F_w} is the extracted feature of a pre-defined feature F_w, I_{F_w} is the CMM dataset to inspect E_{F_w}, $p_{c_{w,u}}$ is a single CMM point of I_{F_w}, and the number of $p_{c_{w,u}}$ is c_{F_w}.

An example of CMM measurement planning for pre-defined features such as plane, cylinder, and free-form surface in a work piece is shown in Fig. 3(a). The point triangulation principle is used to calculate the normal vector of each point for the plane feature as shown in Fig. 3(b). CMM points are retrieved in a cylinder, curvature, and free-form surface feature, by following the path line that represents its geometrical properties [2, 15].

C. Laser Scanning

The scanning process must cover overall surface of a reversed object in which all considered features, F_w and D_ω. Some different views are often being applied to scan overall surface object by changing the position of the object related to the laser scanning source. Let P_l be the scanning position l, where l = 1, 2… L, where L is the number of the scanning position. Pairwise of datasets from different positions, P_1 and P_2, are then aligned and fitted. In this work, two steps registration: rough and fine registration were applied to unify the different laser scanning dataset. These two steps registrations were adopted from our previous work [1, 2].

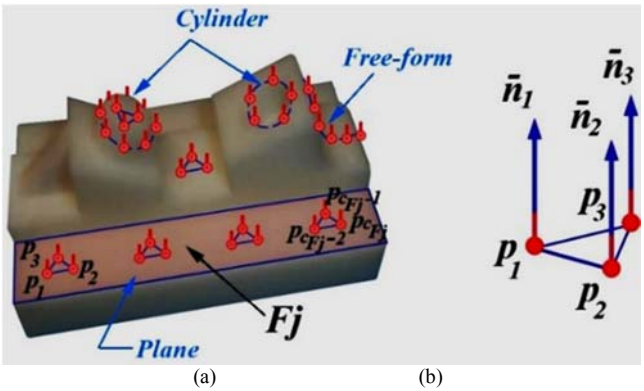

(a) (b)

Fig. 3 Example of CMM measurement planning: (a) CMM measurement planning of plane, cylinder, free-form, (b) CMM triangulation principle and normal vector generation

D. Registration of point cloud datasets to CMM dataset

Basically, alignment and fitting process between point clouds from the registration and CMM dataset is the same as alignment and fitting process between laser scanning datasets. However, the CMM data set is sparse [13, 14] and discrete point dataset while laser scanning are point cloud datasets.

The procedure of the registration between point clouds and CMM dataset is described as follows:

a) CMM dataset is always located in the global coordinate system. The point clouds are aligned onto this position.

b) Selecting the registration references is following the criteria:

- Utilize the datum as registration references.
- The feature extraction can be used to generate the registration references between the point clouds and CMM dataset in both an object with and without datum.
- Grid method can be applied to localize the pairwise dataset in the references area.

c) Correction of the point clouds registration is performed based on CMM dataset.

- Check the distance of all corresponding dataset between the point clouds and the CMM data.
- If the registration error is indicated, the correction of the point cloud error or registration error is executed using the CMM data.
- Optimization (minimization) is performed until the accuracy of the point clouds-CMM registration is statistically fulfilled.

An example of the object with the three-plane datum as the registration references of the point clouds to the CMM dataset is shown in Fig. 4. Based on the procedures, for an object with datum references, the datum can be utilized

directly to be the basis of the registration. The primary, secondary, and tertiary datum of point cloud datasets are aligned and fitted to CMM dataset simultaneously. If the pairwise references are mutually perpendicular, the corresponding point cloud to the CMM data is fitted by minimizing the distance to the references.

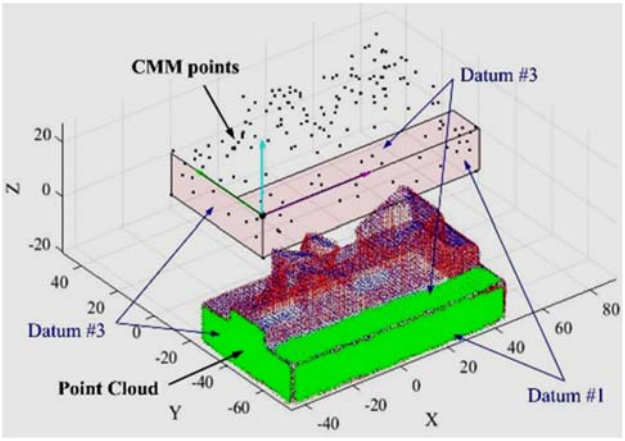

Fig.4. Three plane datum of point clouds and CMM dataset are generated for the registration of point clouds to CMM dataset: green colors are extracted planes from point clouds, and pink colors are extracted planes from CMM dataset

The optimization of fine registration in the references area is achieved by minimizing all plane-point distances between point clouds and its correlated CMM points using the following equation [1,2]:

$$\min e(T,R) = \min \sum_{ITS=1}^{Q} \left| \hat{n}\left(p_{c_{ITS}} - M(T,R).p_{L_{ITS}}\right) \right| \quad (2)$$

where $e(T,R)$ is the error of Euclidian distance of the alignment between the point cloud datasets, $p_{L_{ITS}}$ and the CMM dataset, $p_{c_{ITS}}$ in the intersection region, *ITS*. Q is the number of intersection which is equal to the number of CMM dataset. $\hat{n}$ is the normal direction, and M is the alignment parameters consisting of a translation, T, and a rotation parameter, R.

E. Point Cloud Data Segmentation and Feature Extraction

In the inspection and verification of point cloud registration result, only definitive features can be utilized as an inspected part. In this case, point cloud data segmentation and feature extraction are applied to obtain overall single extracted features from the registration result. The process consists of three main steps: point cloud segmentation, feature extraction and feature verification. Segmentation is performed to cluster point cloud into regions which represent overall single features [5]. This segmentation process is successful if each single extracted feature can represent each correlated pre-define feature. Overall single regions obtained from the segmentation is then extracted to be certain identified features [15]. Next, the extracted features are statistically validated and verified.

In this work, point cloud segmentation is calculated using the region growing approach [2, 5, 6]. Firstly, normal vector and curvature for each point in point cloud are calculated based on its nearest neighbour. Secondly, each point in the point cloud is grouping based on normal vector and curvature using specific threshold value. The output of segmentation is rough segmented regions. Each region is then extracted into a definitive feature. An example of segmentation and feature extraction result is as shown in Fig.5.

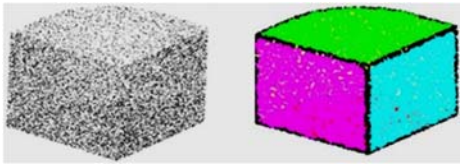

(a) (b)

Fig 5. An example of segmentation result: (a) point cloud data (b) extracted feature result

All the types of extracted features are validated and verified using specific criteria [2]. Plane fitting is employed to confirm and check a planar form, cylinder fitting to validate and verify cylinder form, and line equation to validate and verify points and lines. The Gaussian curvature (K) and Mean curvature (H) are used to validate and verify the ruled-surface form type [15]. There is no sophisticated method to validate and verify the free-form surface. Least square fitting algorithm for feature fitting was proposed in [16] while range data fitting to a primitive feature was proposed in [17]. Verified features which considered as key features are then inspected and verified using CMM data in the next step. The detail of this method of point cloud data segmentation, feature extraction and verification for unstructured point cloud data was discussed deeply in our previous work [2].

F. Feature inspection and verification

Correspondence between a single extracted feature and its CMM control points are localized in grids in which the inspection and verification are performed. Deviation of the feature is calculated based on the error metrics from each single element in the overall grid formed. Next, point cloud registration is then evaluated based on overall single feature deviation.

F1. Grid method reconstruction

A grid method [1, 7] in this work is used to localize the pairwise of the elements of the extracted feature obtained from registration and its CMM control points. Both the point from point cloud dataset, $p_L(x_i, y_i, z_i)$ and the point in the CMM data, $p_c(x_i, y_i, z_i)$ have the x, y, and z coordinate

which represent the grid position. The individual IDs of each point both in the point cloud dataset and the CMM dataset is calculated as follows:

$$IDp_i(x_i, y_i, z_i) = \left(\left\lceil x_{min} - |i|d_g \right\rceil, \left\lceil y_{min} - |j|d_g \right\rceil, \left\lceil z_{min} - |k|d_g \right\rceil\right) \quad (3)$$

where $IDp_i(x_i, y_i, z_i)$ is position of a point in a grid, parameters i, j and k represent ID grid in the x, y and z of the coordinate system, and d_g is grid size.

The grid intersection between the point clouds of an extracted feature and its CMM control point in the same IDs is formulated as follows:

$$ITS_{w,m} = E_{F_w}\big|_{ID_{grid}} \cap \; I_{F_w}\big|_{ID_{grid}} \quad (4)$$

where $ITS_{w,m}$ is the intersection of the point cloud, p_{L_w} of a feature F_w and its CMM control point p_{c_w}, where m = 1, 2, …, c_{F_w}. The number of ITS_w, m is equal to the number of the CMM point control, c_{F_w}.

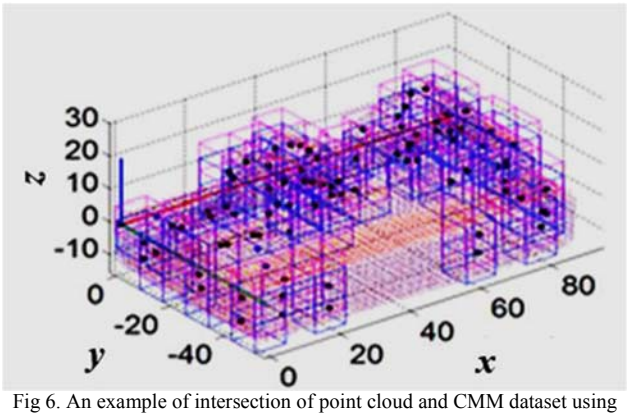

Fig 6. An example of intersection of point cloud and CMM dataset using grid method.

In each intersection, a grid will consist of the element of the considered feature, E_{F_w} and a CMM control point in which the inspection and verification process will be performed. An example of the intersection between a point cloud and a CMM dataset using the grid method is shown in Fig. 6. The method of grid reconstruction in this approach was deeply discussed in our previous work [1].

F2. Distance Error Measurement

The distance error measurement is used to inspect and verify each extracted feature from the point cloud using CMM point in each localized grid. Distance measurement for the plane feature is modified from [7]. There are several conditions of measurement which are used in our schemes such as 3D plane-to-plane distance (d_{Pl-Pl}), 3D point-to-plane distance (d_{p-Pl}), and 3D point-to-point distance (d_{p-p}). Also, the angle between two plane normal vectors θ is measured to control the plane error. Some schemes of the distance measurement are defined as follows:

a. Plane-to-Plane Distance:

Plane-to-plane distance, (d_{Pl-Pl}) is defined as the orthogonal distance between two parallel planes. If a considered plane feature,Pl_{F_w} with the equation $ax + by + cz + d_{Pl} = 0$ and a datum plane, Pl_{D_ω} with the equation $+by + cz + d_D = 0$, the distance between those two parallel planes is formulated as follows:

$$\left(d_{Pl_{F_w}-Pl_{D_\omega}}\right) = \frac{|d_{Pl} - d_D|}{\sqrt{a^2+b^2+c^2}} \quad (5)$$

In this proposed method, the distance between two parallel planes, $(d_{Pl-Pl,m})$ is evaluated based on the grid intersection between the considered plane and its CMM control points to the corresponding datum. The distance of pairwise planes between the datum plane and the inspected plane as shown in Fig. 7. For the m element of considered plane (in each grid), $Pl_{F_{w,m}}$ and its corresponding datum plane P_{D_ω}, the distance of two planes $d_{Pl-Pl,m}$ is formulated as follows:

$$d_{Pl-Pl,m} = Pl_{F_{w,m}}\big|_{m \in ITS_w} - Pl_{D_\omega} \quad (6)$$

where m is the element of the considered plane in a grid, corresponding to the point of CMM data. d_P is coefficient, and ITS_w is the intersection of point clouds of a extracted feature, E_{F_w} and the CMM points, I_{F_w}.

b. Point-to-Plane Distance

The point-to-plane distance, d_{p-Pl} is defined as the orthogonal distance between a CMM point, $p_c$and a plane, Pl as shown in Fig. 7. The distance of the point to the plane in the intersection, m is formulated as follows:

$$d_{p-Pl,m} = \left|p_{c,m} - Pl_{F_w}\right|.cos\alpha\big|_{m \in ITS_w} = \frac{\bar{n}.(p_{c,m} - Pl_{F_w})}{|\bar{n}|}\Big|_{m \in ITS_w} = \frac{ax_i + by_i + cz_i + d_{F_j}}{\sqrt{a^2+b^2+c^2}} \quad (7)$$

where $p_{c,m}$ is a CMM point corresponding with the considered evaluated plane F_w, Pl_{F_w}. $\bar{n}$ is the normal vector of the localized plane. The coefficients a, b, and c are plane coefficients of the plane, and α is the cosine direction of the point about the fit plane.

c. Point-to-Point Distance

The point-to-point distance d_{p-p} is defined as the Euclidian distance between the CMM point p_C ($x_{c_m}, y_{c_m}, z_{c_m}$) and the point of the point cloud $P_L(x_{L_m}, y_{L_m}, z_{L_m})$. The point-to-point distance is formulated as follows:

$$d_{p_L - p_c, m}\big|_{m \in ITS_w} = \sqrt[2]{\left(x_{L_m} - x_{c_m}\right)^2 + \left(y_{L_m} - y_{c_m}\right)^2 + \left(z_{L_m} - z_{c_m}\right)^2}\Big|_{m \in ITS_w} \quad (8)$$

where ITS_w is the intersection between the CMM point and the point of the evaluated feature, F_w.

d. Plane angle

Suppose the equation of the considered plane feature F_w and datum plane reference D_ω are respectively $a_i x + b_i y + c_i z + d_F = 0$ and $a_j x + b_j y + c_j z + d_D = 0$, then the plane angle θ is the normal direction deviation of planes is shown in Fig. 7 and (θ) is formulated as follow:

$$\theta = cos^{-1}\left(\frac{a_i a_j + b_i b_j + c_i c_j}{\sqrt{a_i^2 + b_i^2 + c_i^2}\sqrt{a_j^2 + b_j^2 + c_j^2}}\right) \quad (9)$$

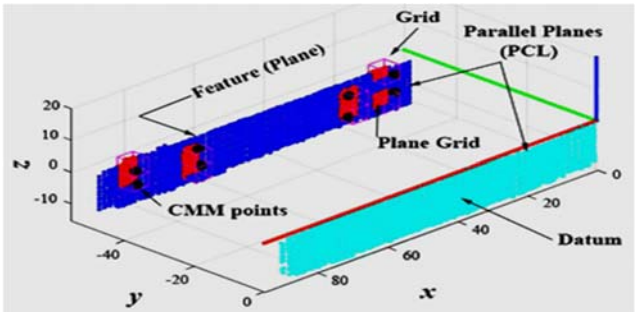

(a)

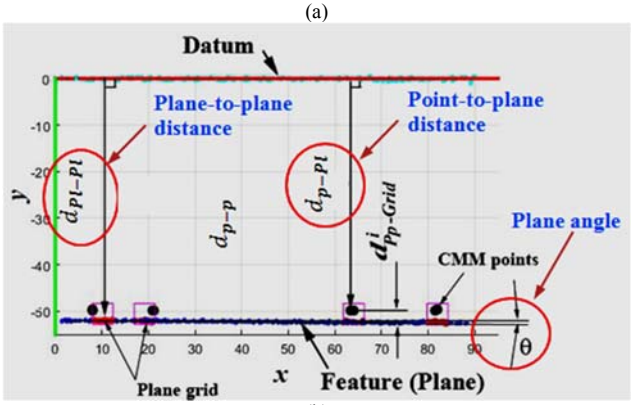

(b)

Fig 7. Distance error measurement scenario: plane-to-plane distance(d_{Pl-Pl}), point-to-plane distance (d_{p-Pl}) and plane angle, θ: 3D views (top) and x-y views (bottom).

G. Correction of the Laser Scanning Datasets

In this step, correction of the registration result can be performed regarding to CMM data points. An example of correction of registration result caused by registration error is shown in Fig. 8.

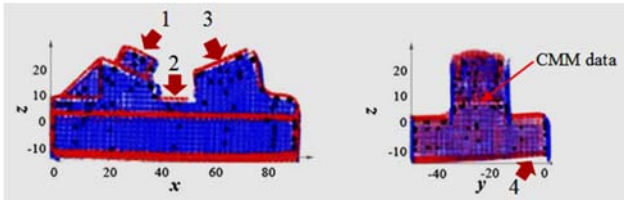

(a)

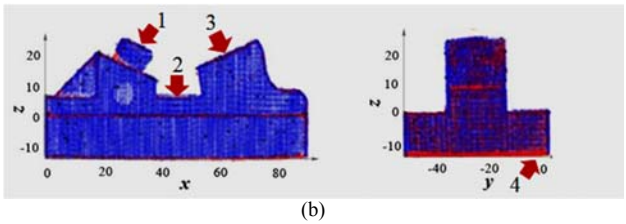

(b)

Fig. 8 Point cloud dataset correction: (a) before correction, and (b) after correction, position 1,2,3 and 4 indicate the error, blue color is point cloud P1, red color is point cloud P2, and the black points are the CMM data

Correction is applied when the error type is appropriately known. The correction process can be implemented using the following steps:

- If the registration error which is caused by registration process, rotation and translation matrices [1, 18] can be applied to correct the position of the laser scanning point cloud to the CMM data. It is discussed in Section 4.4.
- If the registration error which is caused by point cloud dataset error, the following steps can be performed:
  - o If deformation of point cloud related to considered feature is uniform about the datum in the same error value, 3D-scaling can be applied to correct the data. The correction can be in the overall direction (x, y, and z-axis) or partially in only one direction or two directions.
  - o If shear deformation is happening, the data can be corrected using 3D-shearing depending on the direction of the shear deformation.
  - o For non-uniform laser-scan data distortion (if any), interpolation data is applied. This method is not discussed in this paper.
  - o If the deviation is too high, rescanning can be performed.

IV. RESULTS AND DISCUSSIONS

In this work, a 3D printing product is used as shown in Fig. 9(a). This model has three orthogonal plane datum. Pre-defined datum and key features intended to be evaluated are as shown in Fig. 9 (b) and Table 2.

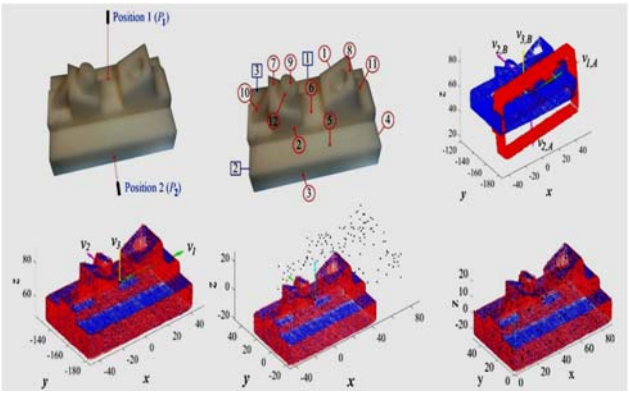

Fig. 9 (a) scanning position, (b) datum and key features identification, (c) initial scanning datasets, (d) rough registration result, (e) fine registration result and CMM dataset, and (f) laser scanning data sets and CMM data points registration result, blue color is point cloud P1, red color is point cloud P2 and the black points are the CMM data

Two scanning positions, P1 and P2, can cover all datum and the key features. The point clouds from both scanning position, P1 with 16,384 points and P2 with 13,096 points, are shown in Fig. 9 (c) and the result of point clouds registration (rough and ICP-fine registration) is shown in Fig. 9 (d). The detail of the registration process of laser scanning datasets is provided in previous paper [1]. The initial position of the point clouds registration and CMM data points are shown in Fig. 9 (e) while the result of the registration of the point clouds to the CMM data points are illustrated in Fig. 9 (f). This registration of the laser scanning datasets and the CMM is using pairwise datum references (see Fig. 6). The next step is evaluating each correlated considered feature (datum and key features) using CMM data points. The grid construction method [1, 7] is applied To localize each intersection of the point cloud and the CMM. The result of the intersection of the laser scanning datasets and the CMM is shown in Fig. 10(a). The segmentation and feature extraction, by segmentation parameters N = 3 (3rd ring), curvature threshold (c_{th}) = 95% and angle of normal (θ_{th}) = 10 degree, is shown in Fig. 10 (b) and Table II.

TABLE II. DATUM AND FEATURE

Features (D_ω or F_w)	Name	Expected feature type	Datum or Features	No. in feature extraction
		Datum references		
D_1	Datum 1	Flat/plane	-	1
D_2	Datum 2	Flat/plane	-	6
D_3	Datum 3	Flat/plane	-	3
		Features		
F_1	Feature 1	Flat/plane	Related to $\#D_1$	10
F_2	Feature 2	Flat/plane	Related to $\#D_1$	8
F_3	Feature 3	Flat/plane	Related to $\#D_1$	5
F_4	Feature 4	Flat/plane	Related to # D_2	13
F_5	Feature 5	Flat/plane	Related to # D_3	7
F_6	Feature 6	Flat/plane	Related to # D_3	15
F_7	Feature 7	Flat/plane	Related to # D_3	61
F_8	Feature 8	Flat/plane	Related to # D_3	22
F_9	Feature 9	Flat/plane	Related to # D_3	20
F_{10}	Feature 10	Flat/plane	Related to # D_3	16

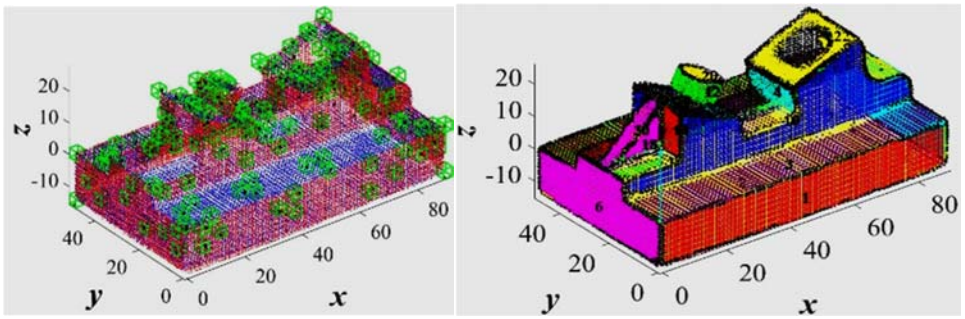

-a -b

Fig. 10. (a) the grid method to localize corresponding laser data points and CMM measurement points, (b) feature segmentation result with the index numbers of main considered features

A1. Evaluation of datum references

Evaluation of datum references is imperative because it influences the validity of the key feature inspection. In this case, three pairwise plane datum references are present: primary, secondary and tertiary datum as shown in Fig. 11. Each feature is evaluated using corresponding CMM data points (points control) in each grid. In this step, automatic computation of the distance between each extracted plane grid to datum reference (d_{Pl-Pl}), called as plane grid to datum, and the distance between the CMM control point and the datum reference (d_{p-Pl}) in each grid. The result of the distance computation of Datum 1, Datum 2 and Datum 3 is shown in Fig. 12.

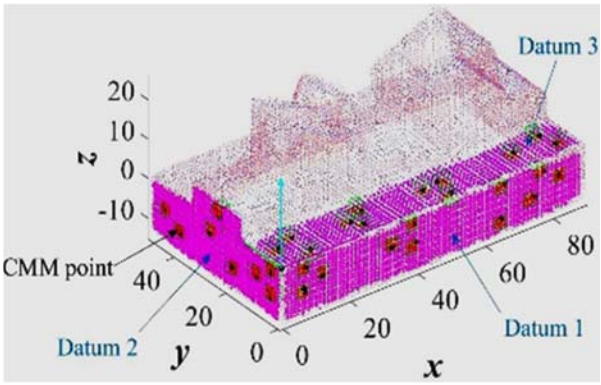

Fig. 11 Datum references evaluation

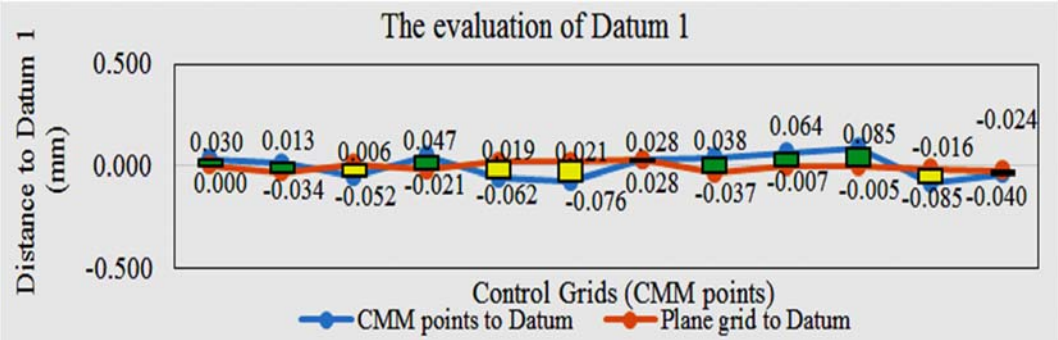

(a)

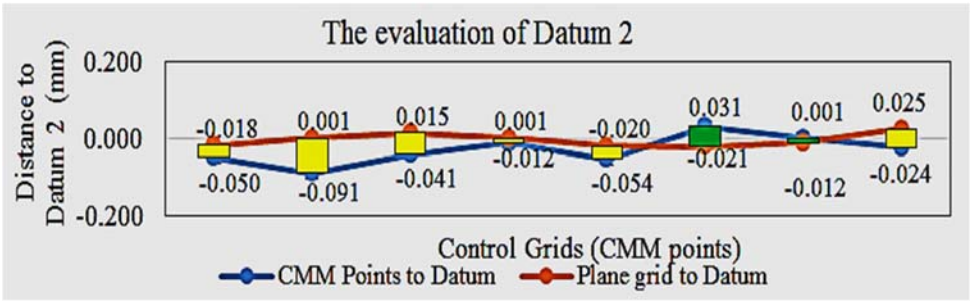

(b), Figure 12 continues on next page.

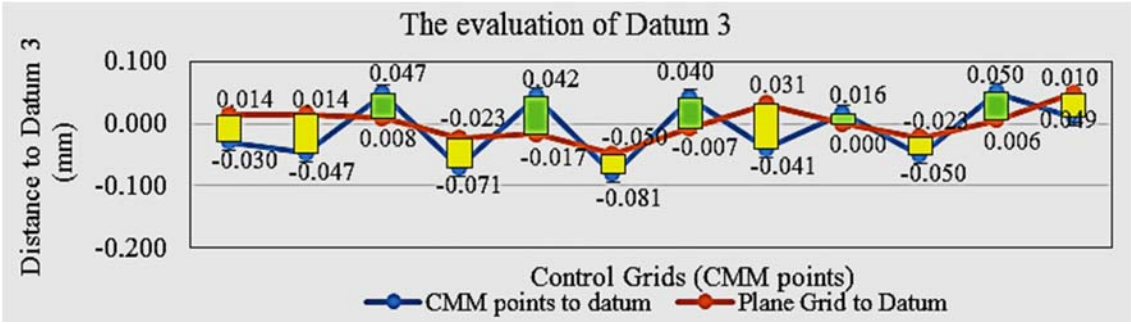

(c)

Fig. 12 Evaluation of extracted Datum Plane by CMM to Datum and Point Grid to Datum Plane: (a) Datum 1, (b) Datum 2 and (c) Datum 3

The differences of distance between plane to datum and control point to datum for each grid are computed and statistically evaluated. The error evaluation for each datum is presented in a mean, a standard deviation, a maximum and a minimum value as shown in Table III.

TABLE III. DATUM EVALUATION

Datum (E_{D_ω})	Point cloud size $(p_{L,w})$	Number of CMM points (c_{D_w})	Differences between CMM points and extracted plane distance in all control grids			
			Mean (mm)	Standard Deviation (mm)	Max (mm)	Min (mm)
Datum 1	3421	12	-0.005	0.068	0.097	-0.090
Datum 2	4154	8	0.026	0.044	0.092	-0.052
Datum 3	1725	12	0.010	0.047	0.071	-0.059

Based on the error evaluation of Datum 1 (primary), Datum 2 (secondary) and Datum 3 (tertiary) as shown in Table 3. The entire extracted datum has small variance (small standard deviation). Therefore, it can be concluded that the pairwise datum has a high degree of confidence and can be used as the basis of the main features inspection.

A2. Evaluation of each extracted key feature

The evaluation of the extracted features of the with-datum product is based on datum references

a) Evaluation Features Related to Datum

Feature 1 (F_1), F_2 and F_3 are plane features which are related to Datum 1 (D_1) as shown in Fig. 13 (a). These features are evaluated based on the distances of the featutes related to Datum 1 (dF_1, dF_2anddF_3) as shown in Fig. 13 (b). The computation result of distance evaluation for features F_1, F_2, and F_3 as the differences between point cloud and CMM data in grids are presented in Table IV.

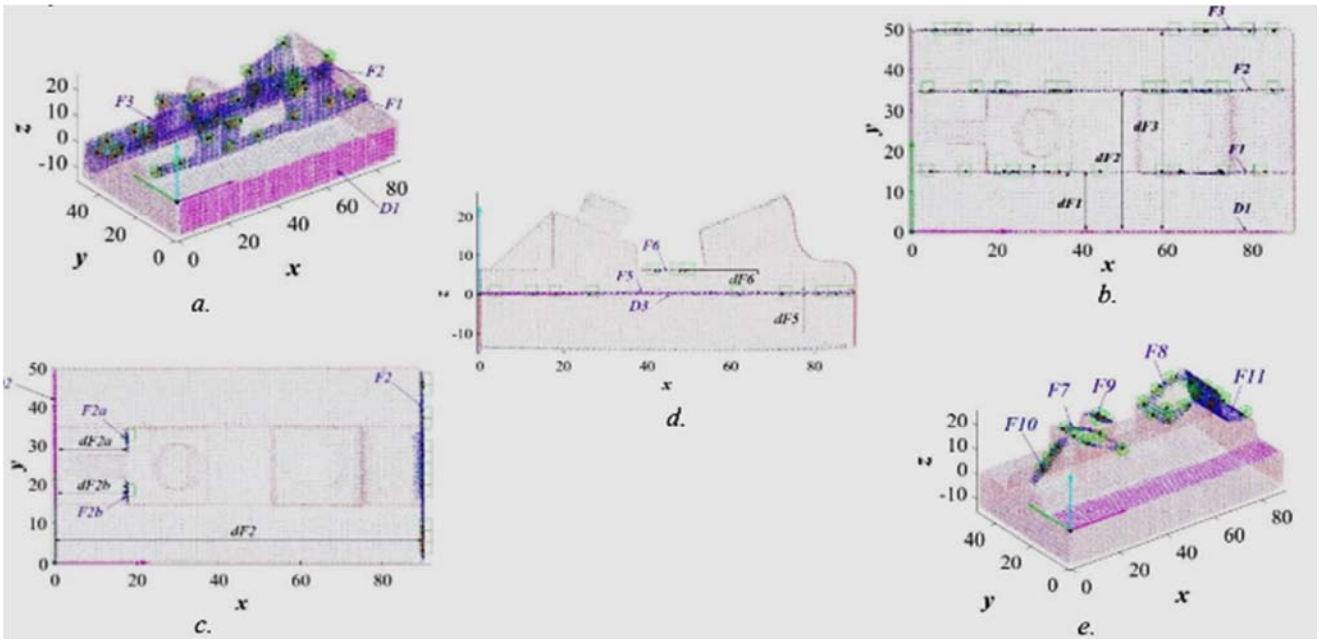

Fig. 13 Evaluation of extracted Key Features: a.) Features related to Datum 1 (3D view), b.) Features related to Datum 1 (2D view), c.) Features related to Datum 2, d.) Features related to Datum 3, and e.) Other features related to Datum 3

Table 4. The evaluation result of Features

Feature (E_{F_w})	*Related to Datum references*	The amount of point cloud ($p_{L,w}$)	The amount of CMM points (c_{D_w})	Differences between CMM points and extracted plane distance in all control grids			
				Mean (mm)	Standard deviation (mm)	Max (mm)	Min (mm)
Feature 1	#D1	2815	12	-0.131	0.062	-0.045	-0.228
Feature 2	#D1	2290	12	-0.149	0.137	0.113	-0.341
Feature 3	#D1	3375	12	0.156	0.203	0.473	-0.131
Feature 4	#D2	3905	12	0.045	0.065	0.132	-0.090
Feature 4a	#D2	45	1	0.017	-	-	-
Feature 4b	#D2	62	1	-0.106	-	-	-
Feature 5	#D3	1991	9	-0.133	0.036	0.205	0.089
Feature 6	#D3	305	6	0.108	0.084	0.080	-0.180
Feature 7	#D3	250	8	0.028	0.084	0.003	-0.031
Feature 8	#D3	461	8	-0.016	0.069	0.069	-0.109
Feature 9	#D3	136	5	-0.070	0.006	0.013	-0.061
Feature 10	#D3	312	3	-0.143	0.095	0.108	-0.076

Based on the position of each grid plane, Feature 1 shows non-parallel trend as shown in Fig. 14 (a) while Feature 2 and Feature 3 tends to shift in the y-direction as shown in Fig 14 (b) and Fig 14 (c), respectively. Both Feature 2 and Feature 3 show deviation, the differences of the distance of Feature 1, Feature 2 and Feature 3 are on average -0.131, -0.149 and 0.156 mm, respectively.

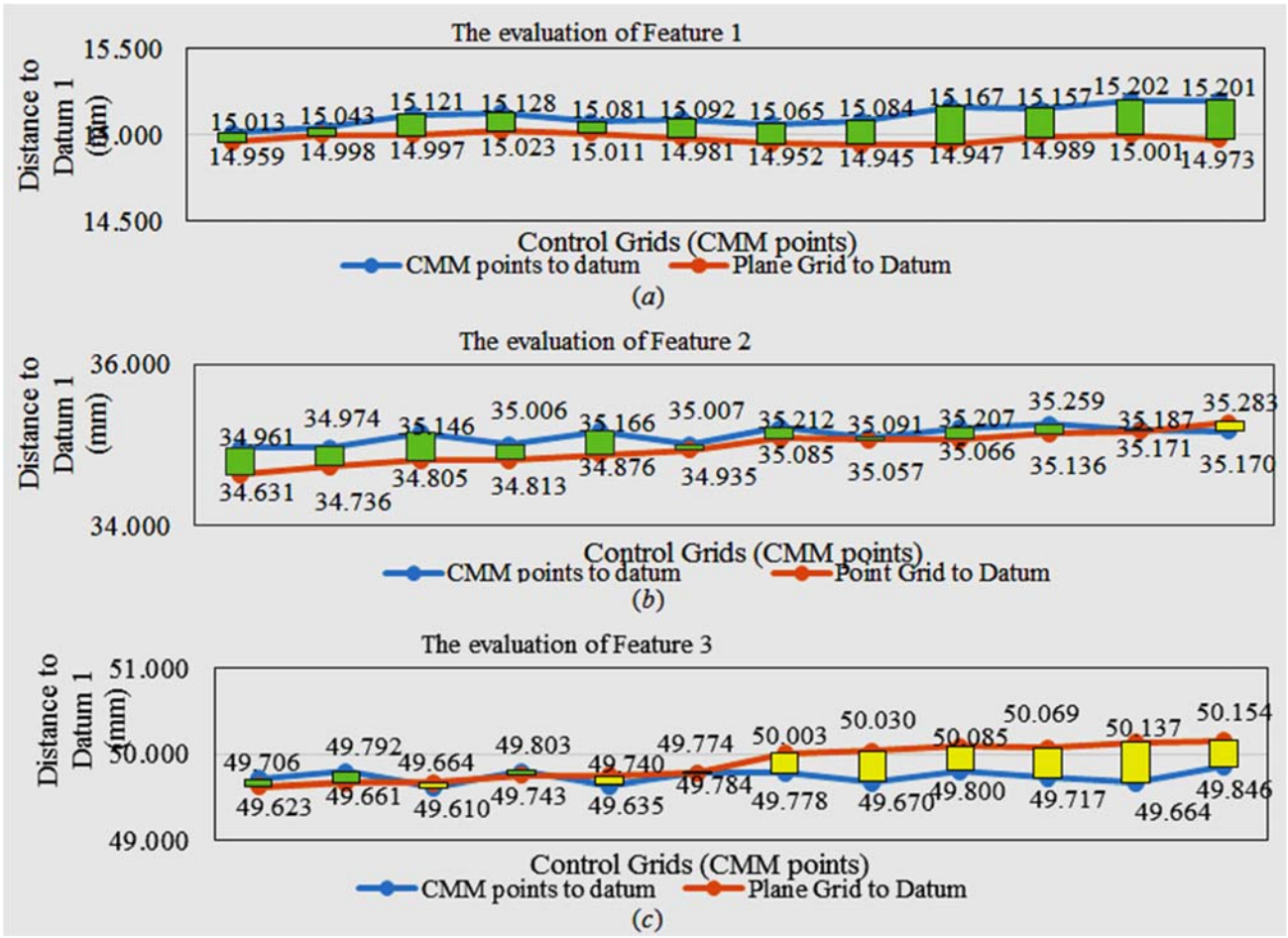

Fig. 14 Evaluation of extracted Datum Plane by CMM dataset: (a) Datum.

b) Evaluation Extracted Features Related to Datum 2

Feature 4 is evaluated based on Datum 2 (D_2) as shown in Fig. 13(c) above. In this case, F_{4a} and F_{4b} are assessed additionally. The result of the evaluation of the extracted plane Features 4 (F_4), Feature 4a (F_{4a}) and Feature 4b (F_{4b}) are shown in Fig. 13 (b) and Table 4. Based on the validation result, the deviation in *x*-direction is calculated to be around 0.045 mm for Feature 4.

c) Evaluation Extracted Features Related to Datum 3

The evaluation of Feature 5 (F_5) and Feature 6 (F_6) is based on the Datum 3 as shown in Fig. 13(d) above. The evaluation results of Features 5 are as shown in Table 4 above. Based on the evaluation result of Feature 5 and Feature 6, it can be concluded the deviation in the *z*-direction is around 0.1 mm.

The valuation of Feature 7 (F_7), Feature 8 (F_8), Feature 9 (F_9), Feature 10 (F_{10}), Feature 11 (F_{11}), and Feature 12 (F_{12}) is as shown in Fig. 13(e) above. Feature 7 (F_7), Feature 8 (F_8), Feature 9 (F_9), and Feature 10 (F_{10}) are the plane features where no datum can be used as feature evaluation reference. Feature 11 (F_{11}) and Feature 12 (F_{12}) are a free-form feature and a cylinder feature, respectively. In this case, we can approach by point-to-point distance correlated with the normal vector of the CMM and the point cloud data. The result of evaluation of Feature 7 (F_7), Feature 8 (F_8), Feature 9 (F_9), Feature 10 (F_{10}), and Feature 11 (F_{11}) are as shown in Table 4 above. It can be concluded that the deviation of Feature 7 to Feature 11 are uniform.

Based on the overall inspection of the extracted features, it is found that the registration yields good result (good alignment and fitting) while the deviation of point cloud datasets is quite uniform in average ± 0.1 mm in the different direction. It can be concluded that the registration accuracy can fulfil the specification because the accuracy of a laser scanner used in this work is 0.1 mm.

V. CONCLUSION

In this paper, a method of inspection and verification of point clouds registration for the reverse engineering was proposed. Point clouds and their registration results are

evaluated by this proposed method based on the inspection and verification each single extracted feature. Each key feature is extracted from point clouds and inspected using CMM data points in each grid constructed. The segmentation, feature extraction, and validation each feature of the main features are carried out automatically. The inspection in each grid is based on plane-to-plane distance error and their plane angle and point-to-plane error, and point-to-to point distance error.

Based on the inspection results of two real cases, it can be concluded that the proposed method can be applied effectively and efficiently in inspection and verification of point clouds registration in reverse engineering practice using the laser scanner. Our proposed method can be applied to evaluate the point clouds registration of reversed products with and without datum. The features such as the plane, cylinder, ruled-surface and free form surfaces can be utilized as pre-defined features to be inspected. This proposed method can enhance more accurate 3D CAD model construction.

This method also has prospective application in the inspection of the registration for different types of datasets. This approach can be implemented in reverse engineering of widely variety product such as mechanical, molding, casting, forging products and so on.

REFERENCES

[1] Muslimin, Jiang Zhu, Hayato Yoshioka, Tomohisa Tanaka, Yoshio Saito, Study on Plane Feature Extraction in Registration of Laser Scanning Data Sets for Reverse Engineering, Journal of Advanced Mechanical Design, Systems, and Manufacturing, Vol. 9, No. 5, 2015. pp. 1-14.

[2] Muslimin, Jiang Zhu, Hayato Yoshioka, Tomohisa Tanaka, Automatic Segmentation and Feature Identification of Laser Scanning Point Cloud Data for Reverse Engineering, Proceeding of ISFA 2015 The International Symposium on Flexible Automation, Cleveland, Ohio, USA, paper no. 21, 2016, pp. 1-8.

[3] Gary K.L. Tam, Zhi-Quan Cheng, Yu-Kun Lai, Frank C. Langbein, Yonghuai Liu, David Marshall, Ralph R. Martin, Xian-Fang Sun, Paul L. Rosin, Registration of 3D Point Clouds and Meshes: A Survey from Rigid to Non-rigid, IEEE Transactions on Visualization and Computer Graphics, Vol. 19, No. 7, 2013, pp. 1199-1217.

[4] Hong Zhou, Yonghuai Liu, Longzhuang Li, Baogang Wei, A clustering approach to free form surface reconstruction from multi-view range images, Image and Vision Computing, Volume 27 Issue 6, 2009, pp. 725-747.

[5] T. Rabbani, F.A. van den Heuvel, G. Vosselman, Segmentation of point clouds using smoothness constraint, In ISPRS Commission V Symposium 'Image Engineering and Vision Metrology', 2006, pp. 248-253.

[6] Gumhold S, Wang X, MacLeod R, Feature extraction from point clouds, In Proc. 10th International Meshing Roundtable, 2001, pp. 293-305.

[7] Xudong Li, Wei Li, Hongzhi Jiang, Huijie Zhao, Automatic evaluation of machining allowance of precision castings based on plane features from 3D point Cloud, Computers in Industry 64, 2013, pp. 1129-1137.

[8] Igor Bešić, Nick Van Gestel, Jean-Pierre Kruth, Philip Bleys, Janko Hodolič, Accuracy improvement of laser line scanning for feature measurement on CMM, Optics and Lasers in Engineering 49, 2001, pp. 1274-1280.

[9] A.Isheil, J.-P. Gonnet, D. Joannic, J.-F. Fontaine, Systematic Error Correction of A 3D Laser Scanning Measurement Device, Optics and Lasers in Engineering 49, 2001, pp. 16-24.

[10] Hsi-Yung Feng, Yixin Liu, Fengfeng Xi, Analysis of Digitizing Errors of A Laser Scanning, Precision Engineering Journal of the International Societies for Precision Engineering and Nanotechnology 25, 2001, pp. 185-191.

[11] Nick Van Gestel, Steven Cuypers, Philip Bleys, Jean-Pierre Kruth, A Performance Evaluation Test for Laser Line Scanners on CMMs, Optic and Laser Engineering 47, 2009, pp. 336-342,

[12] ISO 10360-8: 2013, Geometric Product Specifications (GPS) – Acceptance and re-verification test for Coordinate Measuring Machines – Part 8: CMMs with optical distance sensors, European Committee for Standardization, 2013, pp. 1-59.

[13] V. Carbone, M. Carocci, E. Savio, G. Sansoni and L. De Chiffre, Combination of Vision System and a Coordinate Measuring Machine for Reverse Engineering of Freeform Surfaces, The International Journal of Advanced Manufacturing Technology 17, 2001, pp. 263-271

[14] M. Sokovic, J. Kopac, RE (reverse engineering) as necessary phase by rapid product development, Journal of Materials Processing Technology 175, 2006, pp. 398-403.

[15] P.J. Besl, R.C. Jain, Segmentation through Variable-Order Surface Fitting, IEEE Transaction on Pattern Analysis and Machine Intelligence, Vol. 10, No. 2, 1988, pp. 167-192.

[16] Craig M. Shakarji, Least-Squares Fitting Algorithms of the NIST Algorithm Testing System, Journal of Research of National Institute of Standard and Technology 103, 1998, pp. 633-641.

[17] Soon-Wook Kwon, Frederic Bosche, Changwan Kim, Carl T. Haas, Katherine A. Liapi, Fitting Range Data to Primitives for Rapid Local 3D Modelling using Sparse Range Point Cloud, Automation in Construction 13, 2004, pp. 67-81

[18] J.Y. Lai, W.-D. Ueng, and C.-Y. Yao, Registration and Data Merging for Multiple Sets of Scan Data, International Journal of Advanced Manufacturing Technology, Vol. 15, © Springer-Verlag London Limited, 1999, pp. 54-63.
.